



High-Performance Bio-Based Benzoxazines from Enzymatic Synthesis of Diphenols

Leïla Bonnaud,* Benjamin Chollet, Ludovic Dumas, Aurélien A. M. Peru, Amandine L. Flourat, Florent Allais, and Philippe Dubois

This paper reports the preparation, characterization, and performance of three low viscosity fully bio-based benzoxazine resins synthesized from bio-based furfurylamine, paraformaldehyde, and three new enzymatic originated diphenols obtained through a sustainable and highly selective lipase-catalyzed enzymatic process from *p*-coumaric acid, and three bio-based diols (propanediol, butanediol, and isosorbide, respectively). The enzymatic method is used for the first time, to the authors' knowledge, to design specific diphenolic structures dedicated to the preparation of benzoxazine thermosetting resins whose precursors exhibit easy handling within a wide processing window (from room temperature up to 200 °C). The resulting cross-linked materials present high glass transition temperature ($T_g > 200$ °C) and inherent charring ability upon pyrolysis (≈ 50 wt% at 1000 °C). These results open a valuable and new pathway to develop enhanced benzoxazines and bring them new properties.

1. Introduction

Although the synthesis of 1,3-benzoxazine monomers was first reported in 1944 by Holly and Cope,^[1] benzoxazine resins only enter the field of thermosetting materials in the 90s thanks to Ning and Ishida who popularized their synthesis by a solventless process.^[2,3] These resins present a combination of properties^[4–7] such as high thermal stability, mechanical strength, low flammability, low water absorption, and high chemical resistance that make them of high interest for the preparation of high-performance materials and it is worth highlighting that they appear as one of the rare new polymers which have undergone commercialization in the last decades.^[8] Overall, the attractiveness of benzoxazine resins probably lies on two main additional features: the great flexibility of monomer molecular

design and related chemical functionality^[7] and the great versatility of their synthetic process^[9] though in the industry, only the manufacture in solvent is considered at the present time.

As benzoxazine precursors are readily synthesized by a Mannich-like condensation of an amine, a phenol, and formaldehyde, both the diverse and large number of phenolic derivatives and amine derivatives commercially available allows the preparation of a very wide range of monomers, which can be used in order to tailor or reach specific properties.^[10] The number of newly synthesized monomers is thus constantly increasing with a particular interest for those based on renewable or sustainable organic materials as the development of environmentally compatible and sustainable polymers is one of

the current challenges in polymer science.^[8,11,12]

As aromatic compounds including phenolic derivatives are the second most abundant class of organic compounds in nature representing about 25% of the earth's biomass,^[13] quite a large number of renewable phenol derivatives have been tested in recent years to synthesize benzoxazine precursors such as diphenolic acid,^[14] cardanol,^[15] vanillin,^[16–18] eugenol,^[18–22] chavicol,^[23] guaiacol,^[18,24] “lignin-like” naturally occurring phenolic compounds (coumaric acid, ferulic acid, and phloretic acid),^[18,25] umbelliferone,^[8,26] arbutin,^[27] urushiol,^[28] catechol,^[29] etc. A special interest is focused on difunctional benzoxazine structure because it leads to cross-linking.

Nevertheless, although biomass offers a wide range of phenolic compounds, many are ortho-substituted with a methoxy group leading to benzoxazine precursor configurations that are not favorable to the formation of the cross-linked network required to achieve high performance. To tackle this issue Dumas et al.^[21] proposed a strategy for eugenol-based benzoxazine which consists in substituting parts of ortho-hindered eugenol moieties with free *ortho*-phenol moieties thus leading to precursors bearing mixed moieties and exhibiting an increased number of available reactive sites. This method was further adapted by Puchot et al.^[30] to vanillin-based benzoxazine and generalized under the name of “asymmetric benzoxazine precursor synthesis”.^[31] Another way consists in the copolymerization of the ortho-hindered monomers with other compatible monomers thus favoring an increase of the reactivity of the ortho-hindered monomers instead of their degradation.

Dr. L. Bonnaud, B. Chollet, Dr. L. Dumas, Prof. P. Dubois
Laboratory of Polymeric and Composite Materials
Center of Innovation and Research in Materials and Polymers
Materia Nova Research Center & University of Mons
23 Place du Parc, B-7000 Mons, Belgium
E-mail: leila.bonnaud@materianova.be

A. A. M. Peru, A. L. Flourat, Prof. F. Allais
Chaire Agro-Biotechnologies Industrielles—AgroParisTech
CEBB 3 rue Rouges Terres, 51110 Pomacle, France

The ORCID identification number(s) for the author(s) of this article can be found under <https://doi.org/10.1002/macp.201800312>.

DOI: 10.1002/macp.201800312

This hybrid approach was applied for instance by Dumas et al.^[20] for eugenol-based benzoxazine and by Wang et al.^[24] for guaiacol-based benzoxazines. All these methods based on the use of reactants issued from renewable resources of the abundant biomass represent interesting and promising approaches to decrease the dependence on petro-based resource consumption. However, to further reduce environmental impacts, greener chemical transformation and eco-friendly processes should also be considered.^[32]

In this context, enzymatic syntheses, which usually takes place in mild conditions with reduced waste treatment requirements due to their higher selectivity and lower byproduct generation, are recently gaining increased consideration from the industrial sector as they represent a potential sustainable alternative to classical organic synthesis to achieve new building blocks and polymer materials by a direct valorization of the biomass.^[33] More specifically, lipases appear of particular value for their chemical and thermal stability in solvents, their high substrate selectivity, high yield of transformation of naturally occurring polyols, their ease of handling and recovery as well as recycling as they can be readily immobilized on many substrates.^[34] The use of lipase biocatalyst has been reported in the scientific literature mainly for the production of renewable plate-form ester,^[35] amide^[36] or diphenol molecules for polyester,^[37] poly(ester-urethane),^[38] epoxy resin,^[39] and non-isocyanate polyurethane^[40,41] materials. Especially of interest, Allais et al.^[35] have developed a new methodology for the production of diphenols incorporating lignocellulosic-based monophenolics such as ferulic acid and bio-based diols or diamines through a chemo-enzymatic process involving *Candida antarctica* lipase B (CAL-B, Novozyme 435). This method allows the preparation of diphenolic derivatives whose aromatic rigidity can be balanced by bio-based diol or diamine spacers and which are of particular value in the search for improving the processability of benzoxazine resins. It is worth to note that classical chemistry was already performed by Tüzün et al.,^[42,43] Rao et al.,^[44] and Trejo-Machin et al.^[45] to prepare benzoxazine monomers bearing ester linkages whereas Yagci et al.^[46] and Ishida et al.^[47] have used ether chains. Although they obtained fluid benzoxazine monomers, they could only achieve low glass transition temperature (T_g) polybenzoxazine materials thus limiting their potential use at high temperature. To the best of our knowledge, the enzymatic pathway has not been explored to design specific phenolic structures dedicated to the preparation of 1,3-benzoxazine precursors for high-performance thermosetting applications.

We aim at demonstrating that lipase-mediated biocatalysis is a promising tool to add to the benzoxazine engineering toolbox, which allows for further enlarging the molecular design possibilities of benzoxazine monomers by making available new phenolic structures especially tailored to prepare liquid fully bio-based benzoxazine precursors exhibiting a very large processing window without sacrificing the resulting high thermal and thermo-mechanical performance. More specifically, we report the preparation, characterization, and properties as determined by thermogravimetric analysis (TGA) and dynamic mechanical thermal analysis (DMA) of three new fully bio-based benzoxazine resins synthesized from bio-based furfurylamine, paraformaldehyde, and three new enzymatic originated diphenols (based on *para*-coumaric acid and respectively butanediol, propanediol, and isosorbide).

2. Experimental Section

2.1. Materials

Candida antarctica lipase B supported on acrylic resin, *para*-coumaric acid, isosorbide, 1,3-propanediol, 1,4-butanediol, furfurylamine, and paraformaldehyde were purchased from Sigma-Aldrich and used without any further purification.

2.2. Characterizations

The ¹H NMR spectra were recorded with a NMR spectrometer (Bruker, 500 MHz), using deuterated dimethylsulfoxide (DMSO-*d*₆) as solvent and the chemical shift was calibrated by setting the chemical shift of DMSO as 2.50 ppm.

Calorimetric studies were carried out at a heating rate of 10 °C min⁻¹ using a differential scanning calorimeter (DSC Q200 from TA Instruments) under nitrogen flow of 50 mL min⁻¹. An Indium standard was used for calibration.

Rheological measurements were performed with an ARES rheometer from TA Instruments equipped with a temperature control device with disposable aluminium plate–plate configuration (diameter 40 mm). All experiments were performed in oscillatory mode at a frequency of 1 Hz and 0.5 mm gap between the plates. Two types of measurements were performed. The first test was carried out in temperature ramp mode with a strain of 10%. The samples were placed in the plate–plate geometry assembly and they were heated from 50–220 °C at a heating rate of 3 °C min⁻¹. The storage modulus G' (Pa), the loss modulus G'' (Pa) and the complex viscosity (Pa s) were recorded versus temperature. The second test was performed in isothermal dynamic time sweep mode under a 1% strain. The samples were placed in the plate–plate geometry assembly and they were heated to the target temperature of curing. Measurements started when target temperature was achieved. Two curing temperatures (150 °C and 180 °C) were used for each benzoxazine precursor sample. The storage modulus G' (Pa), the loss modulus G'' (Pa) and the complex viscosity (Pa s) were recorded versus time. Gelation was reached when viscosity diverged toward infinity.

Thermomechanical properties were investigated using a dynamic mechanical thermal analysis (DMA) apparatus (DMA 2980 Dynamical Mechanical Analyzer from TA Instruments). Specimens (60 × 12 × 3 mm³) were tested in a dual cantilever configuration with a dual cantilever length of 35 mm. The thermal transitions were studied in the temperature range of 25–370 °C at a heating rate of 3 °C min⁻¹ and at a fixed frequency of 1 Hz. An amplitude of 10 μm was used corresponding to a strain of 0.043%. One representative sample was used for the measurements. The accuracy of the temperature measurement is ±3 °C.

Thermogravimetric analysis (TGA) was used to study the anaerobic thermal degradation of the cured systems. Approximately 10 mg of the sample was submitted to a temperature ramp from 25–1000 °C at a heating rate of 10 °C min⁻¹ under a nitrogen flow of 60 mL min⁻¹. All TGA experiments were performed by using a TGA Q50 device from TA Instruments.

Fourier transform infrared (FTIR) spectra were recorded in transmission mode using a Bruker IFS 66v/S spectrometer



equipped with a vacuum apparatus. Precursors and cross-linked polymers were powdered and dispersed into a KBr matrix with a weight concentration of about 1 wt%. Spectra were recorded under vacuum from 500–4000 cm⁻¹ with a wavenumber resolution of 4 cm⁻¹. 64 scans were collected for each sample.

2.3. Syntheses

2.3.1. Synthesis of Ethyldehydrocoumarate

Synthesis of ethyldehydrocoumarate (EDC) was performed according to this procedure: *para*-Coumaric acid (30 g, 183 mmol) was dissolved in ethanol (460 mL) and few drops of concentrated hydrochloric acid were added. Reaction was refluxed overnight and cooled to room temperature. The reaction was then put under nitrogen and palladium on carbon (3.4 g) was added and the mixture was vigorously stirred under dihydrogen flux for 24 h. Upon completion, the mixture was filtered over celite and the latter was rinsed with ethanol. Ethanol was removed by distillation under vacuum and the resulting crude mixture was dissolved into ethyl acetate and washed with a saturated aqueous solution of sodium hydrogenocarbonate twice and concentrated. 34.6 g of EDC was recovered (97%) as a pale pink oil.

¹H NMR (CDCl₃): δ (ppm) = 7.03 (d, *J* = 8.1 Hz, 2H) 6.77 (d, *J* = 8.1 Hz, 2H), 4.14 (q, *J* = 7.1 Hz, 2H), 2.88 (m, 2H), 2.61 (m, 2H), 1.24 (t, *J* = 7.1 Hz, 3H)

¹³C NMR (CDCl₃): δ (ppm) = 174.1, 154.4, 132.0, 129.4, 115.4, 60.9, 36.4, 30.1, 14.1

2.3.2. Synthesis of Propane Di-Coumaric Phenol

Synthesis of propane di-coumaric phenol (PDC) was performed according to the following procedure: Propanediol (31 g, 408 mmol), EDC (237 g, 1.22 mol), and *Candida antarctica* lipase B (aka, Novozym 435) (25 g, 10% w/w) were slowly stirred at 75 °C under vacuum for 24 h. At the end of the reaction, the mixture was dissolved in acetone (1 L) and CAL-B was removed by filtration. After flash purification on silica gel (30 μm) with the following gradient: (6/4) cyclohexane/AcOEt to remove excess of EDC then 45/55 to recover PDC, 110 g of PDC was recovered (73%).

¹H NMR (CDCl₃): δ (ppm) = 6.99 (d, *J* = 8.4 Hz, 4H) 6.72 (d, *J* = 8.4 Hz, 4H), 6.57 (s, 2H), 4.00 (t, *J* = 6.3 Hz, 4H), 2.84 (t, *J* = 7.5 Hz, 4H), 2.57 (t, *J* = 6.3 Hz, 4H), 1.85 (m, 2H)

¹³C NMR (CDCl₃): δ (ppm) = 173.8, 154.4, 132.0, 129.4, 115.5, 61.2, 36.1, 30.1, 27.7

2.3.3. Synthesis of Butane Di-Coumaric Phenol

Synthesis of butane di-coumaric phenol (BDC) was performed according to the following procedure: Butanediol (4.9 g, 54 mmol), EDC (31.5 g, 162 mmol), and *Candida antarctica* lipase B (aka, Novozym 435) (3.6 g, 10% w/w) were slowly stirred at 75 °C under vacuum for 16 h. At the end of the reaction, the mixture was dissolved in acetone and CAL-B

was removed by filtration. After flash purification on silica gel (30 μm) with the following gradient: 7/3 cyclohexane/AcOEt to remove excess of EDC then 45/55 to recover PDC and 10/90 to recover BMC (propane mono-coumaric phenol), 17.1 g of BDC was recovered (82%).

¹H NMR (CDCl₃): δ (ppm) = 7.02 (d, *J* = 8.4 Hz, 4H) 6.73 (d, *J* = 8.4 Hz, 4H), 6.17 (s, 2H), 4.02 (m, 4H), 2.86 (t, *J* = 7.5 Hz, 4H) 2.60 (t, *J* = 7.5 Hz, 4H), 1.53 (m, 4H)

¹³C NMR (CDCl₃): δ (ppm) = 173.8, 154.3, 132.1, 129.4, 115.4, 64.2, 36.2, 30.2, 25.1

2.3.4. Synthesis of Isosorbide Di-Coumaric Phenol

Synthesis of isosorbide di-coumaric phenol (IDC) was performed according to the following procedures:

Procedure A: Isosorbide (2.0 g, 13.7 mmol), EDC (10.6 g, 54.7 mmol), and *Candida antarctica* lipase B (aka, Novozym 435) (1.3 g, 10% w/w) were slowly stirred at 75 °C under vacuum for 96 h. At the end of the reaction, the mixture was dissolved in acetone and CAL-B was removed by filtration. After flash purification on silica gel (30 μm) with the following gradient: 7/3 cyclohexane/AcOEt to remove excess of EDC then 45/55 to recover IDC and 10/90 to recover IMC (propane mono-coumaric phenol), 0.7 g of IDC was recovered (11%).

Procedure B: Acetic anhydride (17 mL, 184 mmol) was added dropwise to a stirred solution of 4-hydroxybenzaldehyde (15 g, 123 mmol) in a 1 M aqueous solution of NaOH (150 mL) in a water-ice bath. The resulting mixture was stirred at room temperature for 2 h, and extracted twice with ethyl acetate (100 mL). The combined organic layers were washed with brine, dried over anhydrous MgSO₄, filtered off, and concentrated to dryness to give 4-hydroxybenzaldehyde acetate (19 g, 94%) that was used without further purification.

¹H NMR (CDCl₃): δ (ppm) = 9.92 (s, 1H) 7.85 (d, *J* = 8.7 Hz, 2H), 7.21 (d, *J* = 8.7 Hz, 2H), 2.27 (s, 3H)

2-chloroacetic anhydride (30 g, 175.4 mmol) was added by portion to a stirred solution of isosorbide (10 g, 68.4 mmol) and pyridine (30 mL) in dichloromethane (150 mL) under nitrogen and in a water-ice bath. The resulting mixture was stirred at room temperature for 16 h. The reaction mixture was diluted with dichloromethane (200 mL) and quenched in a water-ice bath with a 1 M aqueous solution of HCl (150 mL). The organic layer was washed with water and brine, dried over anhydrous MgSO₄, filtered off and concentrated to dryness to give bis(2-chloroacetate) isosorbide (17 g, 83%) that was used without further purification.

¹H NMR (CDCl₃): δ (ppm) = 5.25 (m, 2H) 4.88 (t, *J* = 5.1 Hz, 1H), 4.49 (d, *J* = 4.8 Hz, 1H), 4.11 (s, 2 H), 4.05 (s, 2 H), 3.99 (d, *J* = 3 Hz, 2H), 3.9 (t, *J* = 5.1 Hz, 2H)

¹³C NMR (CDCl₃): δ (ppm) = 166.7, 166.5, 85.7, 80.7, 79.3, 75.3, 73.1, 70.5, 40.6, 40.5

Crude bis(2-chloroacetate) isosorbide (32 g, 107 mmol), crude 4-hydroxybenzaldehyde acetate (38 g, 235 mmol) and triphenylphosphine (70 g, 268 mmol) were suspended in a saturated aqueous solution of sodium hydrogenocarbonate (750 mL). The reaction mixture was stirred at 80 °C for 90 min and extracted twice with ethyl acetate (500 mL). The combined organic layers were washed with brine, dried over anhydrous

MgSO₄, filtered off, and concentrated. The crude product was chromatographed on silica gel (30 μm) with the following gradient: 7/3 then 45/55 cyclohexane/AcOEt to give 27.5 g (49%) of an *E/Z* mixture of acetylated IDC-sat.

¹H NMR (CDCl₃): δ (ppm) = 7.75–7.5 (m, 6H), 7.15–7.10 (m, 4H) 7.0 (m, 0.33H) 6.48–6.35 (2d, *J* = 15.9 Hz, 1.69H, 2H vinyl E), 6.05–5.9 (2d, *J* = 12 Hz, 0.33H, 2H vinyl Z), 5.4–5.1 (m, 2.21H), 4.95 (t, *J* = 4.8 Hz, 0.86 H) 4.75 (t, *J* = 4.8 Hz, 0.15H), 4.6 (d, *J* = 4.5 Hz, 0.85H), 4.4 (d, *J* = 4.5 Hz, 0.15H), 4.2–3.7 (m, 4.3H) 2.25 (s, 6H)

¹³C NMR (CDCl₃): δ (ppm) = 169.1, 166.2, 165.8, 152.3, 144.8, 131.9, 131.8, 129.4, 122.2, 117.3, 117.2, 86.0, 81.0, 78.1, 74.2, 73.6, 70.4, 21.2

Piperazine (23 g, 260 mmol) was added to a stirred solution of *E/Z* acetylated IDC-sat (27.5 g, 52.7 mmol) in THF (300 mL) at room temperature. The yellowish mixture was stirred for 2 h and quenched with a 1M aqueous solution of HCl (500 mL) and ethyl acetate (500 mL). The organic layer was washed with water and brine, dried over anhydrous MgSO₄ and filtered off. The filtrate was directly hydrogenated in presence of 10% palladium on carbon (1.5 g) and a H₂ flow at room temperature for 18 h. The reaction mixture was filtered through a pad of celite. The filtrate was concentrated to dryness. The product was triturated with diethylether (100 mL) for 2 h. The resulting white precipitate was collected by filtration to give after drying 20 g of pure IDC (86%, 2 steps).

¹H NMR (DMSO-d₆): δ (ppm) = 9.19 (s, 2H), 7.01 (m, 4H), 6.65 (d, *J* = 8.4 Hz, 4H), 4.95–5.05 (m, 2H), 4.69 (t, *J* = 5.3 Hz, 1H) 4.27 (s, *J* = 5.3 Hz, 2H), 3.8–3.65 (m, 3H), 2.73 (t, *J* = 6.9 Hz, 4H), 2.55 (t, *J* = 6.9 Hz, 4H).

¹³C NMR (DMSO-d₆): δ (ppm) = 172.1, 156.0, 130.8, 130.7, 115.5, 85.8, 80.8, 77.9, 74.1, 72.8, 70.6, 35.9, 35.7, 29.9

2.3.5. Synthesis of Propane Di-Coumaric Phenol-Based Benzoxazine Precursor

Synthesis of propane di-coumaric phenol-based benzoxazine precursor (PDC-Fa) was performed according to the following procedure: in a two-necked round flask of 100 mL, propane di-coumaric phenol (PDC) (0.013 mmol, 4.971 g), furfurylamine (0.028 mmol, 2.7 g), and paraformaldehyde (0.062 mmol, 1.87 g) were dissolved into 6 mL of 1, 4-dioxane under reflux at 120 °C for 7h 30 min. The reaction progress was monitored with thin layer chromatography (silica as stationary phase and 8:2 acetone/toluene as eluent). Then, 1,4-dioxane and the remaining water were evaporated under vacuum at 120 °C and a light yellow oily product was recovered (Yield: 88%). No further purification was carried out. The PDC-Fa precursor was characterized by a *T*_g of ≈19 °C, a polymerization temperature of ≈235 °C as determined by DSC (10 °C min⁻¹), and a charring of 39% at 1000 °C as determined by TGA under nitrogen (10 °C min⁻¹).

2.3.6. Synthesis of Butane Di-Coumaric Phenol-Based Benzoxazine Precursor

Synthesis of butane di-coumaric phenol-based benzoxazine precursor (BDC-Fa) was performed according to the following

procedure: in a two-necked round flask of 100 mL, butane di-coumaric phenol (BDC) (0.013 mmol, 5.004 g), furfurylamine (0.026 mmol, 2.641 g), and paraformaldehyde (0.061 mmol, 1.82 g) were dissolved into 8 mL of 1,4-dioxane under reflux at 120 °C for 7h 30 min. The reaction progress was monitored with thin layer chromatography (silica as stationary phase and 8:2 acetone/toluene as eluent). Then, 1,4-dioxane and the remaining water were evaporated under vacuum at 120 °C and a light yellow oily product was recovered (Yield: 87%). No further purification was carried out. The PBC-Fa precursor was characterized by a *T*_g of ≈15 °C, a polymerization temperature of ≈234 °C as determined by DSC (10 °C min⁻¹), and a charring of 42% at 1000 °C as determined by TGA under nitrogen (10 °C min⁻¹).

2.3.7. Synthesis of Isosorbide Di-Coumaric Phenol-Based Benzoxazine Precursor

Synthesis of Isosorbide Di-Coumaric Phenol-Based Benzoxazine Precursor (IDC-Fa) was performed according to the following procedure: in a two-necked round flask of 100 mL, isosorbide di-coumaric phenol (IDC) (0.011 mmol, 5.006 g), furfurylamine (0.024 mmol, 2.3 g), and paraformaldehyde (0.054 mmol, 1.63 g) were dissolved into 8 mL of 1,4-dioxane under reflux at 120 °C for 7h 30 min. The reaction progress was monitored with thin layer chromatography (silica as stationary phase and 8:2 acetone/toluene as eluent). Then, 1, 4-dioxane and the remaining water were evaporated under vacuum at 120 °C and a light yellow soft and solid product was recovered (Yield: 95%). No further purification was carried out. The IDC-Fa precursor was characterized by a *T*_g of ≈3 °C, a polymerization temperature of ≈236 °C as determined by DSC (10 °C min⁻¹), and a charring of 35% at 1000 °C as determined by TGA under nitrogen (10 °C min⁻¹).

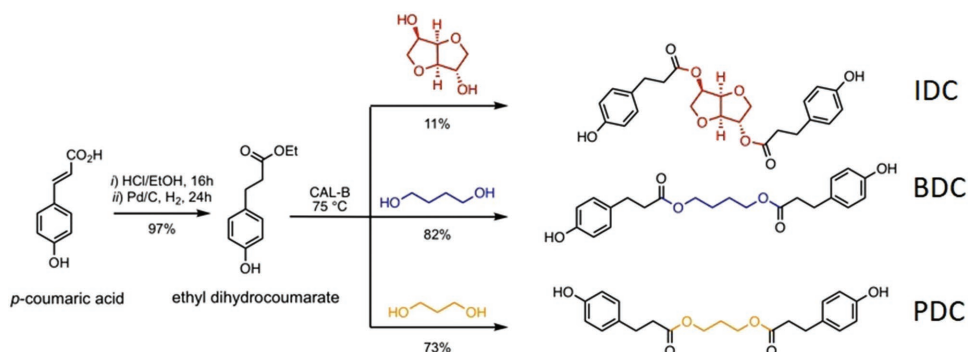
2.3.8. Curing of PDC-Fa, BDC-Fa, and IDC-Fa Resins

The procedure is identical for all the benzoxazine precursors (PDC-Fa, BDC-Fa, and IDC-Fa, respectively). Each of them was introduced in a stainless steel mold, molten, further degassed in a vacuum oven at 140 °C for 10 min, and then step cured in an air-circulating oven according to the following cycle: 2 h at 150 °C, 2h at 180 °C, 3 h at 200 °C, 0.5 h at 250 °C. Thereafter, 60 × 12 × 3 mm³ samples of polybenzoxazines (pPDC-Fa, pBDC-Fa, and pIDC-Fa, respectively) were allowed to slowly cool down to room temperature before their unmolding.

3. Results and Discussion

3.1. Synthesis and Characterization of the Bio-Based Diphenol Reactants and the Corresponding Benzoxazine Precursors

Three bio-based diphenols, PDC, BDC, and IDC, were successfully prepared from *p*-coumaric acid and 1,3-propanediol, 1,4-butanediol, and isosorbide, respectively, following the enzymatic procedure with supported lipase biocatalyst



Scheme 1. Lipase-catalyzed transesterification of ethyl dihydrocoumarate with three different bio-based polyols, namely 1,3-propanediol, 1,4-butanediol, and isosorbide.

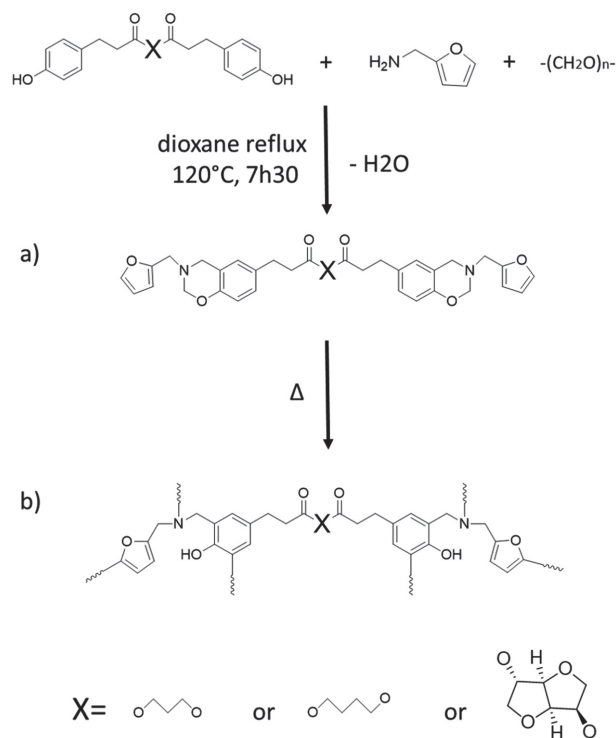
CAL-B summarized in **Scheme 1**. First of all, *p*-coumaric acid was esterified to provide ethyl dihydrocoumarate via a one-pot two-step procedure involving a Fischer esterification and a palladium-catalyzed hydrogenation. Then the solvent-free lipase-mediated transesterifications of ethyl dihydrocoumarate were performed under reduced pressure. Although yields are sensibly lower than those reported with ethyl dihydroferulate^[35] (PDC 73%, BDC 82% and IDC 11% vs PDF 96%, BDF 90% and IDF 87%) starting materials and monoesters can be recovered after purification by flash chromatography or by membrane filtration and reused in further reaction cycles.

Then, these phenols were respectively and successfully reacted with furfurylamine and paraformaldehyde to achieve PDC-Fa, BDC-Fa, and IDC-Fa resin precursors according to the reactions depicted in **Scheme 2**.

The structures of the three products synthesized were investigated and compared to their corresponding reagents, that is, diphenols and furfurylamine, by ¹H NMR. The attribution of the peaks was based on the analysis of ¹H NMR presented in **Figure 1** and on similar benzoxazine derivatives reported in the literature.^[24,27,48–51] For the three products, the well-defined characteristic peaks at about 3.8 ppm and 4.8 ppm corresponding to the protons from Ar-CH₂-N and O-CH₂-N of the oxazine ring respectively attest the formation of the benzoxazine ring. Moreover, the aromatic peaks appearing in the interval 6.5–7 ppm confirm the formation of the heterocycle attached to the benzene ring. Interestingly, the peak at about 9.2 ppm corresponding to the proton from phenolic OH group of the diphenols is not present in the spectra of the benzoxazine precursor achieved evidencing the complete consumption of the reactant. In addition, the signals corresponding to the furan cycle are also observed stressing the preservation of the furan function during the synthesis. More precisely, the protons from the methylene group of furan function are detected at about 3.8 ppm and the protons from furan cycle appear at about 7.6 ppm, 6.4 ppm, and 6.3 ppm.

FTIR analysis was carried out and the spectra of the precursors are displayed in **Figure 2** and compared with the ones of their corresponding diphenols. The main absorbance peaks were identified based on the analysis of the spectra and existing literature on similar structures.^[23,27,48–51] For the three precursors, the characteristic absorption peaks of the benzoxazine ring are observed at 930 cm⁻¹ (C–H out of plane deformation of the

benzene ring attached to the oxazine), 1496 cm⁻¹ (stretching vibrations of the trisubstituted benzene ring, that is, the benzene ring attached to the oxazine ring), 1224 cm⁻¹ (asymmetric stretching of C–O–C), 1010 cm⁻¹ (symmetric stretching of C–O–C), and 1111 cm⁻¹ which is ascribed to the asymmetric stretching vibration peak of C–N–C of the oxazine ring. In addition, the broad bands over 3200 cm⁻¹ which are characteristic of the stretching vibrations of phenolic O–H groups are not observed anymore in the three benzoxazine precursor spectra. This result is in agreement with ¹H NMR data. The C–O–C stretching band of ester functions present on the diphenol moieties should be observed in the interval 1000–1250 cm⁻¹ but it



Scheme 2. Representation of a) the syntheses of the different bio-based benzoxazine precursors PDC-Fa, BDC-Fa, and IDC-Fa from enzymatically synthesized diphenols (respectively, PDC, BDC, and IDC) and b) their proposed cured network structures after polymerization (respectively pPDC-Fa, pBDC-Fa, and pIDC-Fa).

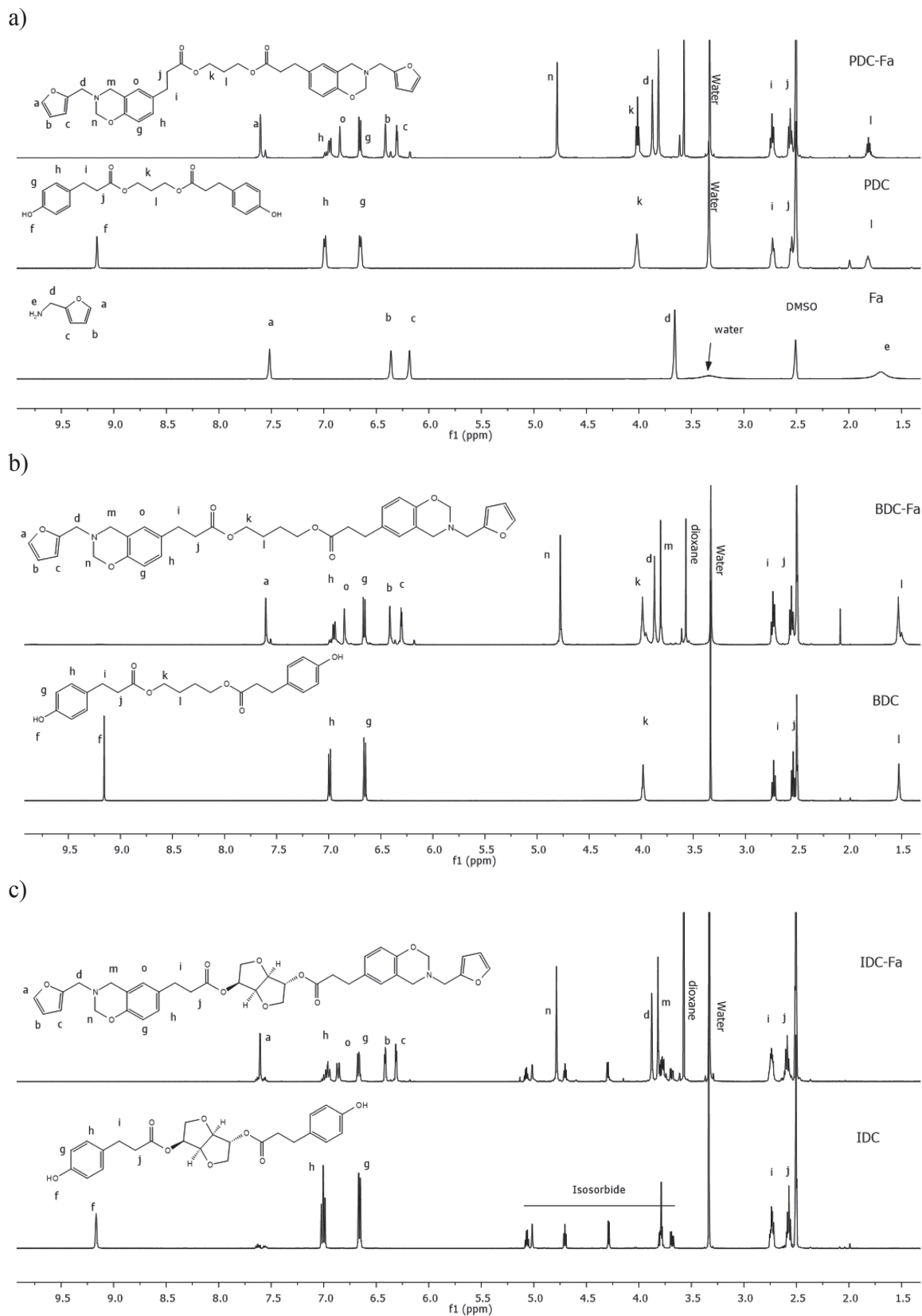


Figure 1. ^1H NMR spectra (DMSO-d_6) of the different bio-based benzoxazine precursors and the diphenols and furfurylamine used for their synthesis a) PDC-Fa, PDC, and furfurylamine b) BDC-Fa and BDC c) IDC-Fa and IDC.

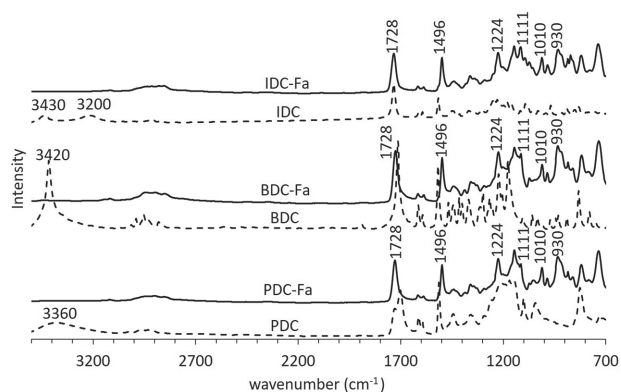


Figure 2. FTIR spectra of the different bio-based benzoxazine precursors, PDC-Fa, BDC-Fa, and IDC-Fa, and their corresponding diphenols: PDC, BDC, and IDC.

is more difficult to identify and assign it in the benzoxazine precursor spectra due to overlapping. Nevertheless, the characteristic peak of carboxyl group from the ester spacer moieties is well detected at about 1718 cm^{-1} for the diphenols and at about 1728 cm^{-1} for the benzoxazine precursors highlighting their formation during the syntheses of the diphenols and their preservation during the benzoxazine syntheses. Finally, the furan group can be observed with the peaks at 1145 cm^{-1} and 981 cm^{-1} . In conclusion, NMR and FTIR analyses allow us to clearly attest the formation of the desired benzoxazine molecule structures.

3.2. Polymerization of the Bio-Based Benzoxazine Precursors

The structural changes with temperature, the reactivity of the three precursors (PDC-Fa, BDC-Fa, and IDC-Fa) and their thermal stability were monitored by DSC and TGA, respectively. Conversely to classical benzoxazine resins, DSC thermograms (Figure 3) show no melting peaks for the three synthesized precursors but three glass transition temperatures (T_g) are observed at $-19\text{ }^\circ\text{C}$ for PDC-Fa, $-15\text{ }^\circ\text{C}$ for BDC-Fa, and $-6\text{ }^\circ\text{C}$ for IDC-Fa. The absence of crystallinity and the low T_g values are good indicators of the processing window broadness of the three resins of this study. Moreover, it is known that 1,3-benzoxazine bearing furan groups exhibit exothermic peaks at temperatures in the range of $200\text{--}300\text{ }^\circ\text{C}$ which are ascribed to the ring-opening polymerization of benzoxazine cycles and the additional participation into the polymerization mechanism of furan moieties resulting in a large exotherm as reported by several authors.^[24,27,48–51] In our case, for the three prepared precursors, two overlapping exothermic peaks with similar maximum temperatures at about $235\text{ }^\circ\text{C}$ and $265\text{ }^\circ\text{C}$ are observed, suggesting there is little influence of the synthesized monomer structure on the curing temperature. However, a closer observation of the onset values of the exothermic peaks seems to indicate that BDC-Fa exhibits a slightly increased reactivity as shown by the lowest value of T_{Ponset} , then comes PDC-Fa, and finally IDC-Fa (Table 1). Moreover, the enthalpy value of the polymerization reaction is found to be smaller in the case of IDC-Fa highlighting its significant lowest polymerizability

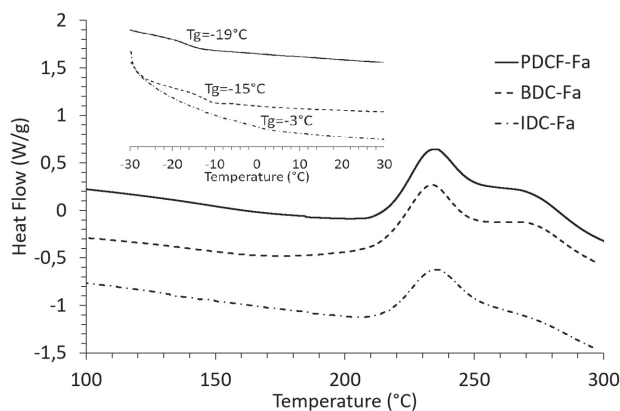


Figure 3. DSC thermograms of PDC-Fa, BDC-Fa, and IDC-Fa benzoxazine precursors.

when compared to PDC-Fa and BDC-Fa (Table 1). More sterically hindered isosorbide spacer of IDC-Fa compared to flexible aliphatic spacers of PDC-Fa and BDC-Fa could limit the molecular mobility and thus explain lower reactivity of IDC-Fa and higher T_g value.

To explore other assumptions, TGA analyses of the three precursors of the study were performed under nitrogen. By TGA, it appears that with temperature the three precursors undergo two main stages of degradation which are presented in Table 1. The first one is observed at about $200\text{--}300\text{ }^\circ\text{C}$ and is attributed to secondary rearrangement reactions linked to the curing process whereas the second one, which is much more prominent, starts at about $430\text{ }^\circ\text{C}$ and is associated to the main degradation of the precursors. It is worth noting that the first degradation step occurs in the same range as the exothermic peak obtained by DSC which corresponds to the curing of the resin. As a result, it partially overlaps the polymerization of the precursors. This phenomenon is found to be more pronounced in the case of IDC-Fa than for PDC-Fa and BDC-Fa as revealed by weight loss values at the temperature of maximum decomposition rate from the first step. This result confirms the lower enthalpy of polymerization measured by DSC in the case of IDC-Fa. Nevertheless, it appears that the weight losses due to the first stage of degradation and recorded by TGA do not affect dramatically the curing of PDC-Fa, BDC-Fa, and IDC-Fa as it proved

Table 1. Thermal properties of PDC-Fa, BDC-Fa, and IDC-Fa benzoxazine precursors obtained by DSC and TGA.

Sample	$T_g^a)$ [$^\circ\text{C}$]	$T_{\text{Ponset}}^b)$ [$^\circ\text{C}$]	$T_{\text{Pmax}}^c)$ [$^\circ\text{C}$]	Enthalpy ^{d)} [J g^{-1}]	$T_{d1}/T_{d2}^e)$ [$^\circ\text{C}$]	Weight loss at $T_{d1}^f)$ [%]	Char ^{g)} at $1000\text{ }^\circ\text{C}$ [%]
PDC-Fa	-19	192	235	247	236/443	8	39
BDC-Fa	-15	180	234	209	235/435	6	42
IDC-Fa	-3	205	236	143	242/442	16	35

^{a)}Glass transition temperature as obtained by DSC; ^{b)}Onset temperature of the exotherm of reaction as obtained by DSC; ^{c)}Maximum temperature of the exotherm of reaction as obtained by DSC; ^{d)}Enthalpy of the exotherm of reaction as obtained by DSC; ^{e)}Temperature of maximum decomposition rate for the first (T_{d1}) and second (T_{d2}) steps as obtained by TGA- N_2 ; ^{f)}Weight loss at the temperature of maximum decomposition rate for the first step as obtained by TGA- N_2 ; ^{g)}Char at $1000\text{ }^\circ\text{C}$ as obtained by TGA- N_2 .

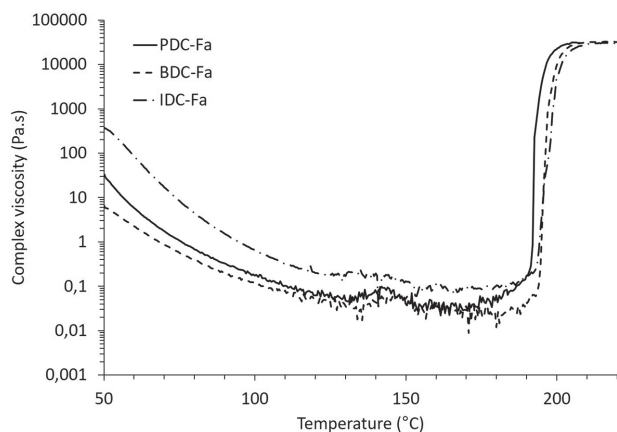


Figure 4. Temperature ramp rheology measurements of PDC-Fa, BDC-Fa, and IDC-Fa benzoxazine precursors.

possible to achieve bulk materials without significant problems and defects. Moreover, these results are in accordance with data reported in the literature for similar types of precursors.^[43,45,50]

To complete DSC and TGA analyses, rheological measurements were performed to further evaluate the polymerization ability of the resins and determine their processing window. Two types of tests were considered. First, the dynamic viscosity profile of the three resins was evaluated as a function of temperature (Figure 4). This is a very effective and rapid way to achieve an overview of the rheological behavior of the resins. Initially, at room temperature, IDC-Fa precursor forms a light-yellow soft solid (382 Pa s at 45 °C) and exhibits higher viscosity than PDC-Fa and BDC-Fa ones, which are pasty liquid (26 Pa s and 5 Pa s, respectively, at 45 °C). As it can be seen in the Figure below, with the temperature increasing, the viscosity of the three resins are found to drop down to about 0.1 Pa s for IDC-Fa precursor and 0.01 Pa s for PDC-Fa and BDC-Fa ones in the temperature area of 125 °C. It is worth noting that PDC-Fa is slightly more viscous than BDC-Fa in the low temperature range (i.e., <125 °C). This important decrease is attributed to the physical precursor softening due to the raising of temperature. In the temperature range 125–180 °C, the viscosity of the three resins remains almost constant with the resins being in a liquid state (0.1 Pa s for IDC-Fa and about 0.01 Pa s for PDC-Fa and BDC-Fa) and finally increases exponentially due to the polymerization and cross-linking of the resins at temperatures higher than 180 °C. It is worth noting that the three resins have a similar behavior at high temperature (i.e., >180 °C) as can be seen with the overlapping of the rheological curves. These results are consistent with DSC results which indicate a close value of the maximum temperature of polymerization for the three resins. It also further highlights the excellent processability of the three resins in a large range of temperatures and the possibility to achieve low viscosity benzoxazine resins.

In addition, isothermal testing at 150 °C and 180 °C under dynamic oscillations of 1 Hz were also performed and resulting storage modulus G' , loss modulus G'' , and complex viscosity were measured as a function of time to evaluate the gelation point of the three resins. Several criteria can be used to define the gelation times. Although some authors consider that in the

Table 2. Isothermal rheology measurements of PDC-Fa, BDC-Fa, and IDC-Fa benzoxazine precursors.

Sample	t_{gelation} at 150 °C [min]	t_{gelation} at 180 °C [min]
PDC-Fa	80	20
BDC-Fa	65	19
IDC-Fa	110	21

case of many systems, the gel point does not always correspond to the crossover point of the shear storage modulus and loss modulus, it is however the most generally accepted criterion.^[52] Another criterion considers that gelation occurs when viscosity increases exponentially to infinity.^[53] The method used in this study to identify the gel point consists in determining the crossover between the tangent line at G' when this curve reaches a value close to 100 000 Pa s and the time baseline. The gel times of the three benzoxazine systems are gathered in Table 2. It can be seen that gel time is shortened at 180 °C when compared to 150 °C. This can be explained by the fact that when temperature increases, molecular mobility also increases leading to accelerated curing. It is also to note that the differences between the three systems are attenuated with increasing temperature and the three benzoxazine systems exhibit almost the same reactivity at 180 °C whereas they present differences at lower temperature. Indeed, at 180 °C the three benzoxazine systems reach about the same viscosity value as shown in Figure 4 and thus exhibit similar gelation time (around 20 min). Conversely, at 150 °C, BDC-Fa which is also the most fluid system is found to be more reactive than PDC-Fa precursor and IDC-Fa system. These results confirm DSC measurements showing a lower onset temperature of polymerization for BDC-Fa (180 °C) when compared to PDC-Fa and IDC-Fa (192 and 205 °C, respectively). For the three resins, we clearly observe a correlation between their viscosity and their reactivity. It is interesting to note that the gelation times of these resins are compatible with composite manufacture processes allowing them to be considered for composite applications.

3.3. Properties of the Bio-Based Cured Polybenzoxazines

Cross-linked polybenzoxazine networks were prepared by curing PDC-Fa, BDC-Fa, and IDC-Fa precursors according to the conditions described in the Experimental Section and led to brown translucent samples pPDC-Fa, pBDC-Fa, and pIDC-Fa, respectively.

To investigate their thermal stability, TGA was carried out under nitrogen. The TGA thermograms indicate very similar results for the three resins as can be seen in Figure 5 and Table 3. Interestingly, all the three resins start to degrade at high temperatures close to 400 °C and they exhibit high charring ability which is promising for fire resistance properties. More precisely, at 800 °C, the char content of the three fully bio-based resins reaches 50 wt%. This result is due to the high content of aromaticity linked to phenolic and furan groups within the structure of the resulting cross-linked materials. Indeed, furan is known to further increase the cross-linking density of

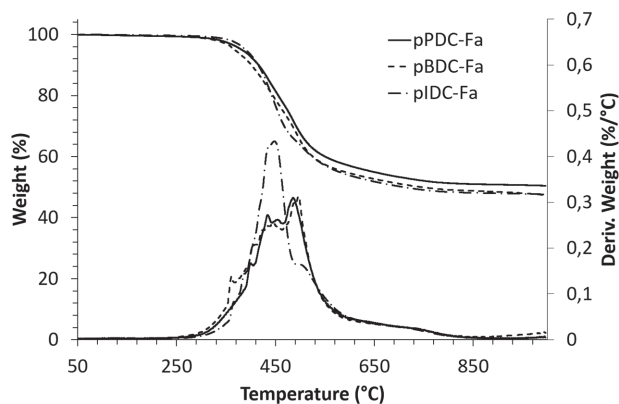


Figure 5. TGA- N_2 thermograms of pPDC-Fa, pBDC-Fa, and pIDC-Fa polybenzoxazines.

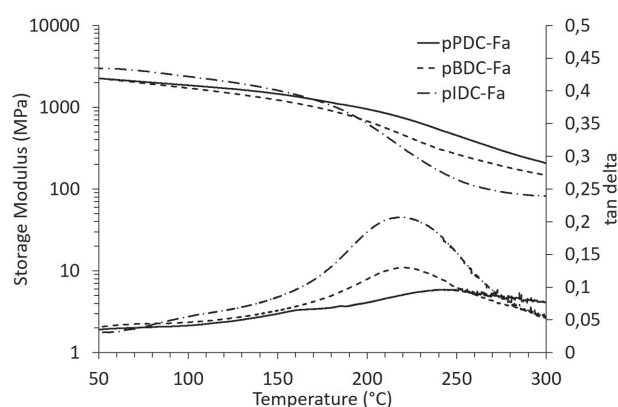


Figure 6. Thermomechanical behavior of pPDC-Fa, pBDC-Fa, and pIDC-Fa polybenzoxazines by DMA analysis.

the cured polybenzoxazines and suppress segmental decomposition into gaseous fragments as the decomposition of polybenzoxazines is usually considered to begin with the cleavage of the amino part.^[54] It is worth noting that such a high charring ability is of high interest for the preparation of more sustainable light-weight structural composite materials for application in transport industries (railway, aeronautic, aerospace for instance...) where high performance represent a prerequisite.

The glass transition (T_g) of the resulting polybenzoxazines were not detected when performing conventional DSC measurements, thus the mechanical transition temperature T_α associated with the T_g was determined using thermomechanical analysis (DMA). The results are shown in **Figure 6** and the data values are summarized in Table 3. It appears that the three cross-linked benzoxazine systems of the study exhibit excellent thermomechanical behavior with high value of T_α (250 °C for pPDC-Fa, 218 °C for pBDC-Fa, and 217 °C for pIDC-Fa) and high storage modulus in the glassy state (2.5 GPa for pPDC-Fa, 2.3 GPa for pBDC-Fa, and 3 GPa for pIDC-Fa). It is also to note that the α transitions are quite large for the three cured systems evidencing heterogeneous network structures which result from several reactions (benzoxazine ring opening polymerization and contribution of furan groups to the curing^[48,51]...). Interestingly, pIDC-Fa material presents the broader and more intense α transition peak. This reveals that pIDC-Fa network is even more heterogeneous than pPDC-Fa and pBDC-Fa and also less cross-linked as confirmed by

Table 3. Thermal and thermomechanical properties of the cured polybenzoxazines.

Sample	$T_{5\%}^a$ [°C]	T_d^b [°C]	Char ^c at 800 °C [%]	T_α^d [°C]	G'_{25}^e at 25 °C [GPa]	G'_{300}^e at 300 °C [MPa]
pPDC-Fa	382	482	51	250	2.5	222
pBDC-Fa	368	495	49	218	2.4	148
pIDC-Fa	395	449	48	217	3.0	100

^a)Temperature of 5% weight loss as obtained by TGA- N_2 ; ^b)Temperature of maximum decomposition rate as obtained by TGA- N_2 ; ^c)Char at 800 °C as obtained by TGA- N_2 ; ^d)Temperature of maximum tan delta peak as obtained by DMA; ^e)Storage Modulus as obtained by DMA.

the lower value of the storage modulus in the rubbery area. This result can also be correlated to previous TGA analysis of IDC-Fa precursors which showed that upon curing this system underwent more secondary degradation reactions which are less favorable for cross-linking. In addition, this result is also in accordance with DSC analysis performed on IDC-Fa precursors showing lowest polymerization when compared to PDC-Fa and BDC-Fa systems upon curing cycle. Anyway, the resulting thermomechanical properties of pPDC-Fa and pBDC-Fa allow them from being considered as one of the most promising high-performance matrices being moreover advantageously fully bio-based and initially liquid thus ensuring an easy processing compared to conventional solid crystalline benzoxazines.

4. Conclusions

To reduce environmental impacts and decrease the dependence on petro-based resource consumption, the development of new monomers fully issued from renewable resources are gaining interest from both the academic and industrial sectors. In the search for high-performance materials, more attention is being paid to the conversion of renewable aromatic biomass into useful precursors such as benzoxazine type especially for the growing thermoset market. Although benzoxazine resins are considered as promising materials, their processability remains a key issue that needs to be addressed in practical use to facilitate their handling and expand their commercial use. Indeed, most available benzoxazine precursors including commercial ones are petro-based solid powders, which exhibit high liquefying temperature that hinders their handling.

Three fully bio-based diphenols combining both high thermal resistance and flexibility were successfully prepared through a sustainable and highly selective lipase-catalyzed enzymatic process from *p*-coumaric acid and three different diols (propanediol, butanediol, and isosorbide, respectively). These new bio-based reactants were further reacted with furfurylamine and paraformaldehyde to manufacture new low viscosity fully bio-based benzoxazine precursors in high yield (about 90%) exhibiting extremely wide processing window

from room temperature up to 200 °C without sacrificing their thermal or thermomechanical performance.

More specifically, these low viscosity benzoxazine precursors allow the formation of highly cross-linked networks involving the participation of the furan group into the polymerization and leading to cured thermosetting materials which exhibit glass transition temperatures higher than 200 °C and present remarkable inherent charring ability upon pyrolysis (about 50 wt% at 1000 °C).

This work demonstrates that *Candida antarctica* Lipase B biocatalysis applied to naturally occurring and renewable phenolic compounds and more generally enzymatic synthesis is a promising and very valuable tool to design new molecular structures especially tailored to bring new properties to benzoxazines.

Acknowledgements

The authors wish to thank the “Région Wallonne” and the European Community for general support in the framework of the Interreg V program (“BIOCOMPAL” project), the Convergence program (“POLYTISS” project), the FEDER 2014–2020 program (“HYBRITIMESURF” and “MACOBIO” projects). They also thank Oltea Murariu for general help in the laboratory and Julie Passion for the additional FTIR analyses. The authors are also grateful to Grand Reims, Département de la Marne, and Grand Est for financial support.

Conflict of Interest

The authors declare no conflict of interest.

Keywords

benzoxazine, bio-based, enzymatic condensation

Received: July 23, 2018

Revised: September 22, 2018

Published online:

- [1] F. W. Holly, A. C. Cope, *J. Am. Chem. Soc.*, **1944**, 66, 1875.
- [2] X. Ning, H. Ishida, *J. Polym. Sci., Part A: Polym. Chem.*, **1994**, 32, 1121.
- [3] H. Ishida, *United State Patent* 5543516, **1996**.
- [4] C. P. R. Nair, *Prog. Polym. Sci.*, **2004**, 29, 401.
- [5] T. Takeichi, T. Kawachi, T. Agag, *Polym. J.*, **2008**, 40, 1121.
- [6] Y. Yagci, B. Kiskan, N. N. Ghosh, *J. Polym. Sci., Part A: Polym. Chem.*, **2009**, 47, 5565.
- [7] H. Ishida, T. Agag, *Handbook of Benzoxazine Resins*, Elsevier, Amsterdam, The Netherlands **2011**.
- [8] C. Rodriguez-Arza, P. Froimowicz, H. Ishida, *RSC Adv.*, **2015**, 5, 97855.
- [9] S. Ohashi, H. Ishida, in *Advanced and Emerging Polybenzoxazine Science and Technology*, Part I (Eds: H. Ishida, P. Froimowicz), Elsevier, Amsterdam, The Netherlands **2017**, Ch. 1.
- [10] N. N. Ghosh, B. Kiskan, Y. Yagci, *Prog. Polym. Sci.*, **2007**, 32, 1344.
- [11] J. Bozell Joseph, M. K. Patel, *ACS Symposium Series*, Vol. 921, American Chemical Society-Division of Cellulose and Renewable Materials, Washington, DC **2006**.
- [12] G. Lligadas, A. Tüzün, J. C. Ronda, M. Galià, V. Cádiz, *Polym. Chem.*, **2014**, 5, 6636.
- [13] J. Gibson, S. C. Harwood, *Annu. Rev. Microbiol.*, **2002**, 56, 345.
- [14] C. Zúñiga, G. Lligadas, J. C. Ronda, M. Galià, V. Cádiz, in *Advanced and Emerging Polybenzoxazine Science and Technology*, Part V (Eds: H. Ishida, P. Froimowicz), Elsevier, Amsterdam, The Netherlands **2017**, Ch. 23.
- [15] S. Shukla, N. Yadav, B. Lochab, in *Advanced and Emerging Polybenzoxazine Science and Technology*, Part V (Eds: H. Ishida, P. Froimowicz), Elsevier, Amsterdam, The Netherlands **2017**, Ch. 24.
- [16] A. Van, K. Chiou, H. Ishida, *Polymer*, **2014**, 55, 1443.
- [17] N. K. Sini, J. Bijwe, I. K. Varma, *J. Polym. Sci., Part A: Polym. Chem.*, **2014**, 52, 7.
- [18] S. Shukla, B. Lochab, in *Advanced and Emerging Polybenzoxazine Science and Technology*, Part V (Eds: H. Ishida, P. Froimowicz), Elsevier, Amsterdam, The Netherlands **2017**, Ch. 25.
- [19] P. Thirukumaran, A. Shakila, S. Muthusamy, *RSC Adv.*, **2014**, 4, 7959.
- [20] L. Dumas, L. Bonnaud, M.-G. Olivier, M. Poorteman, P. Dubois, *Eur. Polym. J.*, **2015**, 67, 494.
- [21] L. Dumas, L. Bonnaud, M. Olivier, M. Poorteman, P. Dubois, *J. Mater. Chem. A*, **2015**, 3, 6012.
- [22] J. Dai, S. Yang, N. Teng, Y. Liu, X. Liu, J. Zhu, J. Zhao, *Coatings*, **2018**, 8, 88.
- [23] L. Dumas, L. Bonnaud, M. Olivier, M. Poorteman, P. Dubois, *Eur. Polym. J.*, **2016**, 81, 337.
- [24] C. Wang, J. Sun, X. Liu, A. Sudo, T. Endo, *Green Chem.*, **2012**, 14, 2799.
- [25] M. Comí, G. Lligadas, J. C. Ronda, M. Galià, V. Cádiz, *J. Polym. Sci., Part A: Polym. Chem.*, **2013**, 51, 4894.
- [26] X. Liu, R. Zhang, T. Li, P. Zhu, Q. Zhuang, *ACS Sustainable Chem. Eng.*, **2017**, 5, 10682.
- [27] L. Dumas, L. Bonnaud, M. Olivier, M. Poorteman, P. Dubois, *Green Chem.*, **2016**, 18, 4954.
- [28] H. Xu, W. Zhang, Z. Lu, G. Zhang, *RSC Adv.*, **2012**, 2, 2768.
- [29] L. R. V. Kotzebue, J. R. de Oliveira, J. B. da Silva, S. E. Mazzetto, H. Ishida, D. Lomonaco, *ACS Sustainable Chem. Eng.*, **2018**, 6, 5485.
- [30] L. Puchot, P. Verge, T. Fouquet, C. Vancaeyzeele, F. Vidal, Y. Habibi, *Green Chem.*, **2016**, 18, 3346.
- [31] P. Verge, L. Puchot, Y. Habibi, in *Advanced and Emerging Polybenzoxazine Science and Technology*, Part I (Eds: H. Ishida, P. Froimowicz), Elsevier, Amsterdam, The Netherlands **2017**, Ch. 7.
- [32] Y. Jiang, K. Loos, *Polymers*, **2016**, 8, 243.
- [33] M. Moura, J. Finkle, S. Stainbrook, *Metab. Eng.*, **2016**, 33, 138.
- [34] Y. Jiang, K. Loos, *Polymers*, **2016**, 8, 243.
- [35] F. Pion, A. F. Reano, P. H. Ducrot, F. Allais, *RSC Adv.*, **2013**, 3, 8988.
- [36] R. Ménard, S. Caillol, F. Allais, *Ind. Crops Prod.*, **2017**, 95, 83.
- [37] F. Pion, P. H. Ducrot, F. Allais, *Macromol. Chem. Phys.*, **2014**, 215, 431.
- [38] M. Z. Oulame, F. Pion, S. Allaudin, K. V. S. N. Raju, P. H. Ducrot, F. Allais, *Eur. Polym. J.*, **2015**, 63, 186.
- [39] A. Maiorana, A. F. Reano, R. Centore, M. Grimaldi, P. Balaguer, F. Allais, R. Gross, *Green Chem.*, **2016**, 18, 4961.
- [40] R. Ménard, S. Caillol, F. Allais, *ACS Sustainable Chem. Eng.*, **2017**, 5, 1446.
- [41] M. Janvier, P. H. Ducrot, F. Allais, *ACS Sustainable Chem. Eng.*, **2017**, 5, 8648.
- [42] A. Tüzün, B. Kiskan, N. Alemdar, A. T. Erciyas, Y. Yagci, *J. Polym. Sci., Part A: Polym. Chem.*, **2010**, 48, 4279.
- [43] A. Tüzün, G. Lligadas, J. C. Ronda, M. Galia, V. Cadiz, *Eur. Polym. J.*, **2016**, 75, 56.
- [44] B. S. Rao, P. Surendra, *Eur. Polym. J.*, **2016**, 77, 139.
- [45] A. Trejo-Machin, P. Verge, L. Puchot, R. Quintana, *Green Chem.*, **2017**, 19, 5065.
- [46] B. Kiskan, B. Koz, Y. Yagci, *J. Polym. Sci., Part A: Polym. Chem.*, **2009**, 47, 6955.



- [47] T. Agag, S. Geiger, S. M. Alhassan, S. Qutubuddin, H. Ishida, *Macromolecules*, **2010**, 43, 7122.
- [48] L. Dumas, L. Bonnaud, M.-G. Olivier, M. Poorteman, P. Dubois, *Eur. Polym. J.*, **2016**, 75, 486.
- [49] C. Wang, C. Zhao, J. Sun, S. Huang, X. Liu, T. Endo, *J. Polym. Sci., Part A: Polym. Chem.*, **2013**, 51, 2016.
- [50] Y. Liu, C. Chou, *J. Polym. Sci., Part A: Polym. Chem.*, **2005**, 43, 5267.
- [51] J. Wang, W. Liu, T. Feng, in *Advanced and Emerging Polybenzoxazine Science and Technology*, Part V (Eds: H. Ishida, P. Froimowicz), Elsevier, Amsterdam, The Netherlands **2017**, Ch. 28.
- [52] H. H. Winter, *Polym. Eng. Sci.*, **1987**, 27, 1698.
- [53] J. M. Laza, C. A. Julian, E. Larrauri, M. Rodriguez, L. M. Leon, *Polymer*, **1999**, 40, 35.
- [54] S. B. Fam, T. Uyar, H. Ishida, J. Hacaloglu, *Polym. Test.*, **2010**, 29, 520.